Photoluminescence in quantum-confined SnO 2 nanocrystals: Evidence of free exciton decay

E. J. H. Lee, C. Ribeiro, T. R. Giraldi, E. Longo, E. R. Leite, and J. A. Varela

Citation: Applied Physics Letters **84**, 1745 (2004); doi: 10.1063/1.1655693
View online: http://dx.doi.org/10.1063/1.1655693
View Table of Contents: http://scitation.aip.org/content/aip/journal/apl/84/10?ver=pdfcov
Published by the AIP Publishing

Photoluminescence in quantum-confined SnO_2 nanocrystals: Evidence of free exciton decay

E. J. H. Lee, C. Ribeiro, T. R. Giraldi, E. Longo, and E. R. Leite[a)]
Laboratório Interdísciplanar de Electroquimica & Cerâmica–Centro Multídisciplinar de Desenvolvimento de Mâteriais Cerâmicos–Departamento de Química, Universidade Federal de São Carlos, Rodovia Washington Luiz, km 235, Caíxa Postal 676, Codigo de Enderecamento Postal 13565-905, São Carlos, São Paulo, Brazil

J. A. Varela
Laboratório Interdísciplanar de Electroquimica & Cerâmica–Centro Multídisciplinar de Desenvolvimento de Mâteriais Cerâmicos–Instituto de Química, Universidade Estadual Paulista, R. Professor Francisco Degni, s/n Araraquara, São Paulo, Brazil

(Received 13 October 2003; accepted 7 January 2004)

Nanocrystalline SnO_2 quantum dots were synthesized at room temperature by hydrolysis reaction of $SnCl_2$. The addition of tetrabutyl ammonium hydroxide and the use of hydrothermal treatment enabled one to obtain tin dioxide colloidal suspensions with mean particle radii ranging from 1.5 to 4.3 nm. The photoluminescent properties of the suspensions were studied. The particle size distribution was estimated by transmission electron microscopy. Assuming that the maximum intensity photon energy of the photoluminescence spectra is related to the band gap energy of the system, the size dependence of the band gap energies of the quantum-confined SnO_2 particles was studied. This dependence was observed to agree very well with the weak confinement regime predicted by the effective mass model. This might be an indication that photoluminescence occurs as a result of a free exciton decay process. © *2004 American Institute of Physics.*
[DOI: 10.1063/1.1655693]

Research on semiconductor quantum dot (QD) systems has been of great interest for the last several years. This is mainly due to novel physical and chemical properties displayed by these nanometer-scale structures. The extensive experimental and theoretical studies done on III–V (e.g., GaAs and InP) and II–VI (e.g., Cd chalcogenides) semiconductors resulted in solid knowledge of the theory of QDs.[1–3] Recently, there has been growing interest in the properties of wide-band gap oxide QD semiconductors, such as nanocrystalline SnO_2. This size-dependent linear and nonlinear optical properties are desirable for applications such as photonic devices and UV-lasing systems. Several studies have reported the optical properties of SnO_2 QDs, but none has presented photoluminescent emission related to free exciton decay, which is necessary for application to UV-lasing systems.[4–7] On the other hand, luminescence related to free exciton decay in bulk SnO_2 has already been reported.[8]

When the dimensions of nanocrystalline particles approach the exciton Bohr radius (a_B), a blueshift in energy is observed due to the quantum confinement phenomenon. The effective mass model is commonly used to study the size dependence of optical properties of QD systems. In this approach the exciton is treated analogously to a hydrogen atom, but is limited by spatial confinement. Therefore the energy of the system is obtained by solving the proper Schrödinger equation. In this manner two regimes are defined according to the coupling of motion of the electron and the hole in the exciton: weak and strong confinements. In the former the particle size is larger than a_B, and the electron and the hole are treated as a correlated pair. The blueshift of the band gap energy is described by Eq. (1), where E_g^{eff} is the effective band gap energy, E_g is the bulk band gap energy, R is the particle radius, $\hbar$ is the Planck constant over 2π (i.e., approximately 1.0546×10^{-34} J s in MKS units), and μ is the effective reduced mass.

$$E_g^{\text{eff}} = E_g + \frac{\hbar^2\pi^2}{2\mu R^2}. \tag{1}$$

In the latter, the QD radius is below a_B, the electron and hole motion is not correlated and the shift in the band gap energy is given by Eq. (2), calculated by the variational method given by Brus,[9]

$$E_g^{\text{eff}} = E_g + \frac{\hbar^2\pi^2}{2\mu R^2} - \frac{1.8e^2}{\varepsilon R} + \cdots. \tag{2}$$

Tin dioxide has bulk band gap energy E_g of 3.6 eV, static dielectric constant ε of approximately 14 and the effective reduced mass μ may be replaced by the electron effective mass ($m_e^* = 0.275m_0$), since $m_e^* \ll m_h^*$ (m_e^* and m_h^* are the electron and hole effective masses, respectively).[8,10] Therefore the calculated electron Bohr radius a_B is approximately 2.7 nm. In this work we demonstrate the size dependent photoluminescence properties of SnO_2 nanocrystals and the good agreement between the blueshifts in energy predicted by the effective mass model and the experimental results. The results indicate that the luminescence emitted is related to a free exciton decay process.

Details of the experimental procedure to obtain SnO_2 nanocrystals is described elsewhere.[11] The synthesis reaction

a)Author to whom correspondence should be addressed; electronic mail: derl@power.ufscar.br

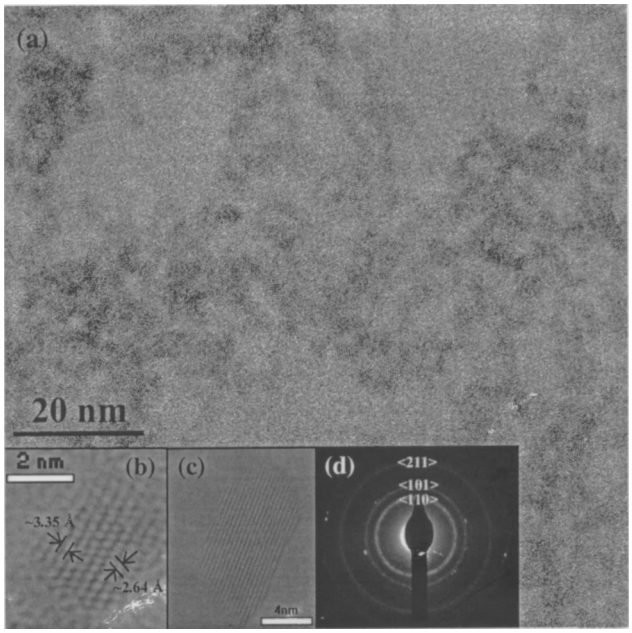

FIG. 1. TEM characterization: (a) Low magnification TEM image overview; (b) HRTEM image of an isolated nearly spherical nanoparticle; (c) HRTEM image of an elongated grown particle, and (d) SAD pattern of an agglomeration of nanoparticles. The SAD pattern can be indexed to the rutile phase of SnO_2.

consisted of the hydrolysis of $SnCl_2\ 2H_2O$ (Mallinckrodt) in ethanolic solution (Merck absolute ethanol). This procedure enables one to obtain nanocrystalline SnO_2 at room temperature. Cleaning of the chloride ions was performed by dialysis in de-ionized water. The final product is a colloidal suspension of nanocrystalline tin dioxide, which we further refer to as pure synthesized SnO_2. Nanocrystals of different sizes were synthesized by making small changes in the procedure. First, the addition of surfactant tetrabutyl ammonium hydroxide (TBA, aqueous solution 0.4 M from J. T. Baker) enabled us to obtain smaller particles, since its stereochemic and electrostatic effects prevented particle growth by the grain rotation induced grain coalescence (GRIGC) mechanism.[11–13] The product of this synthesis procedure will be referred to as TBA-added SnO_2. In order to prepare particles of larger size, hydrothermal treatment was carried out at 200 °C for different periods of time (5, 24, 48 and 100 h). The dependence of the photoluminescence properties on the particle size was studied using six specimens. The morphology and particle size distribution were characterized by a 200 kV transmission electron microscope (Philips CM200). The samples for transmission electron microscopy (TEM) were prepared by wetting carbon-coated copper grids with a drop of the colloidal suspensions for 20 s, followed by drying in air. Photoluminescence (PL) spectra were collected by a Jobin-Yvon, Inc. Fluorolog model FL3-12 fluorimeter. A Xe lamp was used for excitation with the photon wavelength fixed at 250 nm. The PL spectra were collected in the 250–400 nm range with a photomultiplier tube detector. Optical spectra in the ultraviolet and visible light ranges (UV-vis) were collected by Perkin-Elmer equipment. All optical measurements were done in the colloidal suspensions at room temperature.

Figure 1 shows high-resolution transmission electron microscopy (HRTEM) images and a selected-area diffraction (SAD) pattern of the pure synthesized SnO_2 nanoparticles. The SAD patterns of all the samples were characteristic of polycrystalline samples and could be indexed to the rutile structure of the cassiterite phase of tin dioxide. From the HRTEM images it can be observed that there are two types of morphology displayed by the nanoparticles: (1) nearly spherical and (2) elongated oriented particles. The presence of elongated oriented particles is an indication that particle growth occurs by the GRIGC mechanism. The TBA-added SnO_2 sample had a smaller mean particle radius and almost no elongated particles at all, due to the stereochemic and electrostatic effects of TBA. Table I presents the values of the mean particle radii, which were estimated from the particle size distributions obtained by measurement of over 200 particles in the TEM images. The lower left inset of Fig. 1 shows a HRTEM image of an isolated nearly spherical tin dioxide particle. The separation between lattice planes estimated from this image was approximately 3.35 Å, which corresponds to the {110} plane family, and 2.64 Å, which can be ascribed to the {101} plane family. Figure 1(c) illustrates a SnO_2 nanoparticle with an elongated morphology due to hydrothermal-induced growth.

TABLE I. Effect of modification in the experimental procedure on the mean particle radius and effective band gap energy of SnO_2 nanoparticles.

Specimen	Mean particle radius (nm)	Effective band gap energy (eV)
Purely synthesized	1.75	4.01
TBA added	1.50	4.05
Hydrothermal 200 °C/5 h	1.99	3.94
Hydrothermal 200 °C/24 h	2.59	3.71
Hydrothermal 200 °C/48 h	4.26	3.69
Hydrothermal 200 °C/100 h	4.16	3.68

The results of optical characterization are displayed in Fig. 2. It can be observed from the UV-vis measurements [Fig. 2(a)] that the TBA-added sample shows a blueshift at the onset of absorption, compared to the purely synthesized sample. The opposite occurred for the hydrothermally treated samples. This effect can readily be ascribed to the effect of particle size (i.e., a quantum confinement phenomenon), since the mean particle size is close to the value of the exciton Bohr radius. The same behavior can be seen in the photoluminescence characterization [Fig. 2(b)]. The decrease in particle radius created a blueshift in the photon energy emitted. The PL spectra consisted of single broad bands peaked at energies greater than the bulk band gap energy for all samples. The PL was recorded up to 400 nm, and no other band could be observed. Previous work in the literature has reported PL emission at energies below 3 eV, indicating that the emission process did not occur by free exciton electron-hole recombination. It is usually thought that no band-to-band transition luminescence is observed due to the presence of point defects, such as oxygen vacancies.[6,7]

Assuming that the maximum intensity photon energy in the PL spectra corresponds to the band gap energy, it was possible to study the effect of the particle radius on the band gap energy of the samples (Table I). This assumption is quite reasonable, since we are interested in observing the behavior of the mean particle size. Figure 3 shows the experimental and theoretical size dependence of the effective band gap

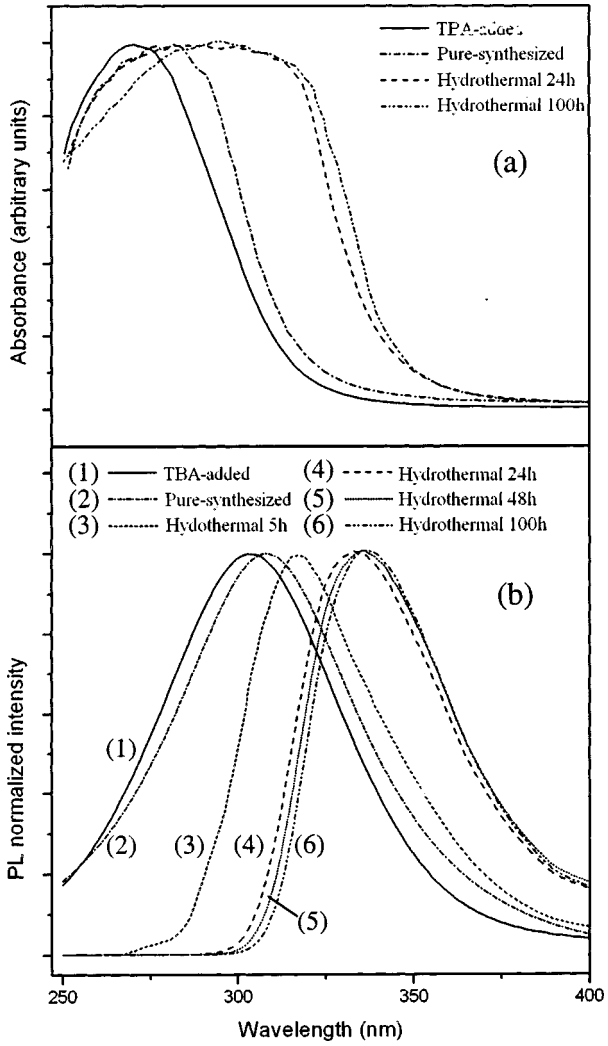

FIG. 2. Optical characterization of the SnO_2 colloidal suspensions: (a) Absorbance spectra measured by UV-vis of nanoparticles of different size and (b) photoluminescence emission spectra of excitation of $\lambda = 250$ nm. All measurements were carried out at room temperature.

energy. It can be observed that there is very good agreement between the experimental results and the theoretical predictions. Most of the samples fit the weak confinement regime curve very well. The main difficulty in separating the weak and strong confinement limits in SnO_2 is due to the relatively small exciton Bohr radius compared to that in most II–VI and III–V semiconductors. Some of the samples presented a mean particle radius close to that of the exciton Bohr radius. In this region the confinement regimes do not behave significantly different and both fit the experimental data well. To observe characteristic strong confinement behavior it would be necessary to prepare smaller particles, which is very difficult. The effective mass model assumes that a blueshift in the band gap energy occurs due to spatial confinement of an exciton. Hence to generate a free exciton, energy higher than the effective band gap energy must be available. In the absence of additional levels introduced by defects, radiative electron-hole recombination of this free exciton should result in photon emission with energy equivalent to the band gap energy. Therefore, the agreement between the predictions of

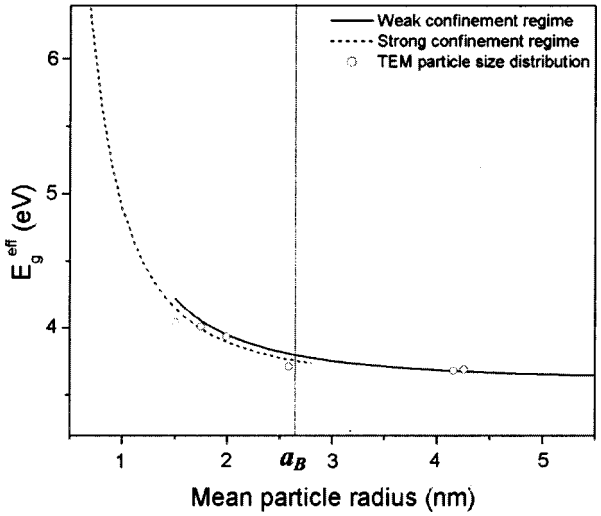

FIG. 3. Experimental and theoretical predictions of the behavior of the band gap energy as a function of the QD size. Experimental mean particle sizes were estimated from TEM images. The exciton Bohr radius (a_B) separates the strong and weak confinement regimes.

this model and the experimental results indicates that the PL observed for the SnO_2 QDs is related to a free exciton decay process.

The nanocrystalline tin dioxide particles prepared in this work showed PL emission compatible with the needs of UV-lasing application. The size dependence of the PL emitted photon and the band-to-band (free exciton decay) luminescence are desired characteristics for this kind of application, since it would be possible to tailor the lasing wavelength. The size dependence behavior of the band gap energy indicated that the photoluminescence occurred due to a free exciton decay process. It was also shown that it is possible to have a certain amount of control over the particle size of QDs. Further studies on the growth mechanisms of SnO_2 nanoparticles are currently being done in order to enable the production of these quantum dots.

The authors would like to acknowledge the Brazilian funding agencies FAPESP and CNPq.

[1] S. V. Gaponenko, *Optical Properties of Semiconductor Materials* (Cambridge University Press, Cambridge, 1998), Chaps. 2 and 3.
[2] T. J. Bukowski and J. H. Simmons, Crit. Rev. Solid State Mater. Sci. **27**, 119 (2002).
[3] N. N. Ledentsov and D. Bimberg, J. Cryst. Growth **255**, 68 (2003).
[4] B. Yu, C. Zhu, and F. Gan, Opt. Mater. (Amsterdam, Neth.) **7**, 15 (1997).
[5] X. Wu, B. Zou, J. Xu, B. Yu, G. Tang, G. Zhang, and W. Chen, Nanostruct. Mater. **8**, 179 (1997).
[6] N. Chiodini, A. Paleari, D. DiMartino, and G. Spinolo, Appl. Phys. Lett. **81**, 1702 (2002).
[7] F. Gu, S. F. Wang, C. F. Song, M. K. Lü, Y. X. Qi, G. J. Zhou, D. Xu, and D. R. Yuan, Chem. Phys. Lett. **372**, 451 (2003).
[8] V. F. Agekyan and Y. A. Stepanov, Sov. Phys. Solid State **34**, 266 (1992).
[9] L. Brus, J. Phys. Chem. **90**, 2555 (1986).
[10] K. J. Button, C. G. Fonstad, and W. Dreybrodt, Phys. Rev. B **4**, 4539 (1971).
[11] E. R. Leite, T. R. Giraldi, F. M. Pontes, E. Longo, A. Beltran, and J. Andrés, Appl. Phys. Lett. **83**, 1566 (2003).
[12] R. Lee Penn and J. F. Banfield, Science **281**, 969 (1998).
[13] D. Moldovan, V. Yamakov, D. Wolf, and S. R. Phillport, Phys. Rev. Lett. **89**, 206101 (2002).